JPET # 260497

Title Page

Modest Blood-brain Barrier Permeability of the Cyclodextrin Kleptose®: Modification by Efflux and Luminal Surface Binding

WA Banks, Kory Engelke, Kim M. Hansen, Kristin M. Bullock, Pericles Calias

Geriatric Research and Clinical Center, Veterans Affairs Puget Sound Health Care System, Seattle, Washington (WAB, KMH, KMB)

Division of Gerontology and Geriatric Medicine, Department of Medicine, University of Washington School of Medicine, Seattle, Washington (WAB)

Tunnell Consulting Inc, 900 E Eighth Ave, Suite 106, King of Prussia PA 19406 (KE)

Cerecor, Inc, 540 Gaither Road, Suite 400, Rockville, MD 20850 (PC)

JPET Fast Forward. Published on July 18, 2019 as DOI: 10.1124/jpet.119.260497
This article has not been copyedited and formatted. The final version may differ from this version.

Running Title Page: BBB permeability of cyclodextrin

Corresponding author: William A Banks, 810/1, VAPSHCS, 1660 S. Columbian Way, Seattle, WA 98108, phone: 206 764 2701; wabanks1@uw.edu

No of Text pages: 14

Number of Tables: 3

Number of Figures: 7

Number of References: 34

Number of Words for Abstract: 228

Number of Words for Introduction: 514

Number of Words for Discussion: 1250

Nonstandard Abbreviations:

API: Active Pharmaceutical Ingredient

BBB: Blood-brain Barrier

CD: Cyclodextrin

Kleptose, Klep: (2-Hydroxy-[2-14C]propyl)-β-cyclodextrin

I-Alb: Albumin radioactively labeled with 125I

Tc-Alb: Albumin radioactively labeled with 99mTc

Expt: Exposure Time

Ki: Unidirectional Influx Rate

Recommended Section: Drug Discovery and Translational Medicine

Abstract

Cyclodextrins (CD) have a variety of uses from acting as excipients to aiding the ability of lipid soluble drugs to cross the blood-brain barrier (BBB). They are being investigated as an active pharmaceutical ingredient (API), most recently for the treatment of Niemann-Pick disease, a lysosomal storage disease. Cyclodextrins are helpful in animal models of and human subjects/patients afflicted with Neimann-Pick disease, including improving the neurological component of the disease. The improvement in brain disease by intravenous administration implies that cyclodextrins can cross the BBB, but there are only a few studies that have directly addressed this. In the current studies, multiple-time regression analysis indicated that the 2-hydroxypropyl-β-cyclodextrin (kleptose ®; Klep) radioactively labeled with 14C (C-Klep) crossed the BBB at a slow rate by a non-saturable mechanism consistent with transcellular diffusion. However, the rate of transport varied greatly by brain region with no detectable uptake by spinal cord; additionally, many regions rapidly reached equilibrium between brain and blood. The presence of a brain-to-blood efflux system was also detected and much of the C-Klep did not completely cross the BBB, but loosely adhered to the luminal surface of brain endothelial cells. Peripheral tissues also took up C-Klep with the kidney taking up the most, consistent with renal clearance. In conclusion, we demonstrated minimal uptake of the β-cyclodextrin kleptose by brain with accumulation being affected by efflux and reversible luminal binding.

Significance statement: This cyclodextrin which produces therapeutic effects on the central nervous system after peripheral administration penetrates the BBB poorly.

JPET Fast Forward. Published on July 18, 2019 as DOI: 10.1124/jpet.119.260497
This article has not been copyedited and formatted. The final version may differ from this version.

Uptake by brain to a therapeutic level will likely be difficult to achieve without giving high peripheral doses, bypassing the BBB, or otherwise altering penetration into brain.

Introduction

Cyclodextrins (CDs) are cone-shaped oligosaccharides used in an increasing number of therapeutic situations (Loftsson and Brewster, 2010). With a hydrophobic inner surface and a hydrophilic outer surface, CDs are able to bind to hydrophobic molecules or to cap the hydrophobic regions of molecules, resulting in a more water-soluble complex.

Originally, CDs were used as excipients, improving the delivery of small molecules such as prostaglandins (Davis and Brewster, 2004). This excipient property has been extended to peptides and proteins, with the CD capable of binding to the functional groups of the amino acids (Varca et al., 2010). CDs have been postulated to aid in the systemic delivery of peptides and proteins after oral or nasal administration (Soares et al., 2007). Nasal delivery when administered high at the level of the cribriform plate can result in uptake by brain (Frey, 2002). Peptides combined with CDs can have an altered distribution pattern in brain, raising the possibility that they may be useful in targeting specific regions (Nonaka et al., 2008; Nonaka et al., 2012).

More recently, CDs have been attributed to have direct pharmacologic actions. One such effect is for CDs to facilitate the clearing of cholesterol from cells. In both animal models of and patients with Niemann-Pick disease, an autosomal recessive lysosomal storage disease that results in accumulation with cells of cholesterol and glycosphingolipids, 2-hydroxypropyl-β-cyclodextrin trademarked as Kleptose ® (Klep), results in significant removal of cholesterol from liver and decreased hepatosplenomegaly (Davidson et al., 2009; Liu et al., 2009; Matsuo et al., 2013). In mice, peripheral administration of the CD results in reduced intraneuronal storage of cholesterol and

JPET Fast Forward. Published on July 18, 2019 as DOI: 10.1124/jpet.119.260497
This article has not been copyedited and formatted. The final version may differ from this version.

glycoshingolipids, decreased neuroinflammation, less neurodegeneration, and significant prolongation of life (Davidson et al., 2009; Liu et al., 2009). In humans, peripheral administration resulted in measurable but less spectacular improvements in brain function (Matsuo et al., 2013).

The above studies would show that peripheral administration of CDs can result in improvement of CNS symptoms. This, in turn, would suggest that CDs have the potential to cross the blood-brain barrier (BBB) (Calias, 2017). Several studies have shown that drugs complexed with CD can enter the CNS as well as cross other membrane barrier membranes, including the BBB (Gil et al., 2012; Conceicao et al., 2017). However, there are few studies that have examined the ability of CDs themselves to cross the BBB. Using an in vitro model of the BBB consisting of primary brain endothelial cells, Monnaert (Monnaert et al., 2004) found that several CDs crossed the BBB . The rate of passage varied over 4-fold and the effects of modifications with methylation or hydroxypropylation were variable and not predictable. In vivo studies in mice have found large distribution volumes in brain after the peripheral administration of radioactive CD (Pontikis et al., 2013). Because those distribution volumes did not increase over time as is typical of blood-to brain transport, it was proposed that the uptake by brain represented binding to the luminal surface of brain endothelial cells, a rare, but documented cause of false positives for the gold standard techniques which they used (Triguero et al., 1990; Maness et al., 1994).

Here, we quantified the degree to which intravenously administered radioactive Klep [2-Hydroxy-[2-14C]propyl)-β-cyclodextrin] can cross from blood into whole brain, brain regions, and spinal cord. We also evaluated its ability to cross in the brain-to-blood

direction, its uptake by peripheral tissues, its reversible binding to the luminal surface of the BBB, and its sequestration by brain endothelial tissues.

Materials and Methods:

Radioactive Materials: Kleptose [(2-Hydroxy-[2-14C]propyl)-β-cyclodextrin] that was radioactively labeled with 14C (C-Klep) was obtained from Institute of Isotopes Co Ltd (Budapest, Hungry). Specific activity was (0.251 MBq/mg). Bovine serum albumin was obtained from Sigma-Aldrich (St. Louis, MO) and was labeled with 125I using the chloramine-T method (I-Alb) or with 99mTc (Tc-Alb) and purified on a column of Sephadex G-10.

Tissue Uptake

Multiple-time regression analysis (Blasberg et al., 1983; Patlak et al., 1983): Male mice averaging about 30 g in body weight were anesthetized with ip urethane and the left carotid artery and the right jugular vein exposed. Mice were given an injection into the jugular vein of 200 μl of lactated Ringer's solution containing 106 dpm of a 14C-labeled kleptose. Blood from the carotid artery was obtained and the mice then immediately decapitated at the time points of 1, 2, 3, 4, 5, 7.5, 10, 20, 30 min with n = 2/time point for a total of 18. The brain (frontal cortex, parietal cortex, occipital cortex, hippocampus, hypothalamus, thalamus, striatum cerebellum, midbrain, pons-medulla, olfactory bulb) and spinal cord (cervical, thoracic, and lumbar) were dissected and weighed and serum

JPET Fast Forward. Published on July 18, 2019 as DOI: 10.1124/jpet.119.260497
This article has not been copyedited and formatted. The final version may differ from this version.

obtained as above, levels of radioactivity determined, and results expressed as brain region/serum ratio in units of μl/g. Values for whole brain were calculated by summing values for the above brain regions (the olfactory bulb.) The peripheral tissues or portions thereof (kidney, spleen, heart, gastrocnemius muscle, liver, lung) were obtained and weighed and the levels of radioactivity expressed as μl/g. The tissue/serum ratios were plotted against exposure time (Expt, in min), which was calculated as:

$$\text{Expt} = \frac{\left[\int_0^t \text{Cp}(\tau)\text{d}\tau\right]}{\text{Cpt}}$$

Where t is the time between the intravenous injection and sampling, Cp is the cpm/ml of arterial serum, Cpt is the cpm/ml of arterial serum at time t, and τ is the dummy variable for time. The slope of the linear portion of the relation of tissue/serum ratio vs Expt measured the unidirectional influx rate (Ki in units of μl/g-min).

Other mice (n=20) were given injections as above, except that half the mice (n=10) had 30 mg of unlabeled kleptose included in the jugular injection. Tissues were collected as above, results expressed as μl/g, and groups compared by Student's t-test.

Other mice anesthetized with urethane were given an injection into the jugular vein of lactated Ringer's solution containing 106 cpm of I-Alb. Brain and peripheral tissues were obtained, weighed, and radioactive levels determined as above at 1, 2, 5, 10, 20, and 30 min after the injection. As these values did not change over time, they were combined across time and the mean tissue/serum ratio subtracted from the ratio for C-Klep and multiplied by 100 and by the dose of C-Klep injected to yield the percent of the injected dose taken up per g of tissue (%Inj/g).

Other mice (n = 19) anesthetized with urethane were given an injection into the jugular vein of 200 μl of lactated Ringer's solution containing 106 dpm of C-Klep and 106 cpm of Tc-Alb. Ten min after the iv injection, the abdomen and thorax were opened, blood collected from a nick in the abdominal aorta, and the jugular veins severed. In 10 mice, 20 ml of cold lactated Ringer's solution infused into the left ventricle of the heart, thus washing out the vascular space of the brain, whereas 9 mice did not receive washout. Levels of 99mTc and 14C were determined in whole brain and arterial serum and expressed as brain/serum ratios.

Brain-to-Blood Passage

Brain-to-blood efflux rates were assessed by the intracerebroventricular) injection method (Banks and Kastin, 1986; Banks et al., 1986). Mice were anesthetized with an ip injection of 0.15ml of 40% urethane (Sigma-Aldrich, St. Louis, MO). The scalp was removed and a hole was made into the skull (0.5mm posterior and 1mm lateral to the bregma) and 1μl of lactated Ringers solution containing 2.5x104 DPM of C-Klep with or without unlabeled Klep (0.15 mg/mouse) was injected into the lateral ventricle of the brain using a 1.0 μl Hamilton syringe. Ten min after the icv injection, blood was obtained from the carotid artery and the mice decapitated. The whole brain was removed and weighed. The amount of C-Klep available for transport at t = 0 was estimated in mice that had been overdosed with urethane and had been dead for 10-20 min before receiving the C-Klep (Banks and Kastin, 1989; Banks et al., 1997). Solvable (1.5 ml) was added to the brain or to 0.50 ml of the arterial serum and incubated overnight at 60 oC, 15 ml of

ecoscint added, and each sample counted for 60 min a beta counter. The amount of C-Klep that was transported out of the brain (%T) was determined with the equation:

$$\%T = [100(cpm/g)0 – (cpm/g)10]/(cpm/g)0$$

where (cpm/g)0 is the mean level of cpm/g for the t=0 group and (cpm/g)10 is the individual mouse's level of cpm/g at t = 10 min. The appearance in blood of C-Klep 10 min after icv injection was expressed as the cpm in a ml of arterial serum divided by the amount injected multiplied by 100 and designated as %Inj/ml.

Octanol/Buffer Coefficient

About 40,000 dpm of C-Klep were placed into a test tube containing 500 uL of octanol and 500 uL of phosphate buffered saline placed on top. The two phases were vigorously mixed for 1min and the test tube centrifuged for 10 min at g at 4 oC. An aliquot from each of the two phases was carefully removed and the level of radioactivity determined. The results were expressed as the ratio of the dpm in the octanol phase divided by the dpm in the buffer phase.

Capillary Depletion

The capillary depletion method was used to separate cerebral capillaries and vascular components from brain parenchyma. Mice were anesthetized with an intraperitoneal injection of 0.15 mL of 40% urethane. Mice received an injection of 1x106 cpm Tc-Alb with 2x106 dpm C-Klep in 0.2 mL LR and 10 min later, 5 mice underwent washout as

outlined above and 4 did not have washout. The whole brain was homogenized in glass with physiological buffer and mixed thoroughly with 26% dextran. The homogenate was centrifuged at 5400g for 15 min at 4°C. The pellet, containing the capillaries, and the supernatant, representing the brain parenchymal/interstitial fluid space, were carefully separated. Radioactivity levels in the capillary pellet, the brain supernatant, and the arterial serum were determined for both Tc-Alb and C-Klep and expressed as capillary/serum and brain parenchyma/serum ratios. The C-Klep ratios were corrected for vascular contamination by subtracting the corresponding ratios for Tc-Alb; these results are reported as the delta capillary/serum ratio and the delta brain parenchyma/serum ratio.

Statistics

Calculations and comparisons of regression lines were performed using Prism 6.0 (GraphPad Inc, San Diego, CA). Two means were compared by Student's t-test and more than two means were compared by Analysis of Variance (ANOVA) followed by Newman-Keuls range test. Means are reported with their standard error term and n.

Results

Figure 1 shows the relation between serum concentration and time after IV injection. An early phase (2-10 min) with a half-life disappearance of 15.7 min was followed by an equilibrium phase. The volume of distribution (Vd) for the first ten

minutes after injection as calculated from the antilog of Figure 1 (lower panel, linear line) was 24.8%Inj/ml or about 4.0 ml.

C-Klep crossed the BBB with a unidirectional influx rate (Ki) of 0.236 +/- 0.057 μl/g-min (Fig 2, upper panel; Table I). The percent of the IV administered dose taken up per g of brain formed a hyperbolic curve with time and had a theoretical maximal value of 0.072 +/- 0.006, reaching steady state about 10 min after IV injection (Fig 2, lower panel).

C-Klep entered all regions of the central nervous system, including the olfactory bulb and all regions of the spinal cord (Fig 3). Ki is calculated using only the linear portion of the tissue/serum vs exposure time ratio; the filled circles in figure 3 show the data points used to calculate Ki, while the open circles were excluded because they departed from linearity. Brain regions varied over 10-fold in their rates of uptake for C-Klep. The region with the fastest uptake was the hypothalamus with a Ki of 0.757 +/- 0.155 μl/g-min and the region with the slowest uptake was the frontal cortex with a Ki of 0.062 +/- 0.018 μl/g-min. The occipital cortex, hypothalamus, cerebellum, thalamus, and midbrain reached equilibrium during the course of the study, whereas the other brain regions continued to accumulate C-Klep throughout the study.

Tissue/serum ratios correlated with exposure for all peripheral tissues except heart, indicating active accumulation by these tissues (Figure 4). Lung had the fastest uptake and quickly reached steady state. Spleen had the slowest uptake. Of the tissues with measurable accumulation, only spleen and kidney did not reach steady state during the study.

In order to express results as %Inj/g, we needed to measure and correct regions for vascular space. The results for the vascular spaces are shown in Table II. Figure 5 shows the results for %Inj/g. Olfactory bulb and hypothalamus had the highest uptake rates, whereas frontal cortex had the least. For peripheral tissues, kidney had the highest uptake, whereas liver had the lowest value for %Inj/g. Although heart did not have a measurable Ki, its tissue/serum values for C-Klep exceeded those for vascular space and so had a measurable value for %Inj/g; likely it reached equilibrium so quickly that the Ki could not be measured with the approach taken here. The %Inj/g corrected for albumin space was negative for the 3 spinal cord regions (n = 18): Cervical: -0.1 +/- 0.04; Thoracic -0.04 +/- 0.01; Lumbar: -0.004 +/-0.02.

Neither whole brain nor any brain region exhibited evidence for inhibition with the dose of 30 mg/mouse of unlabeled Klep (Fig 6). Serum showed a trend towards a decrease and kidney showed a dramatic uptake.

The octanol/buffer coefficient is a measure of lipid solubility and correlates with the ability of substances to cross the BBB by the mechanism of transcellular diffusion (el Tayar et al., 1991). The octanol/buffer coefficient for C-Klep was (1.3 +/- 0.1)10-3 (n = 6) for which the log value is (-)2.89. Results for washout of whole brain is shown in Table 3. Tc-Alb results showed that the washout removed >90% of the vascular contents. However, the brain/serum ratio for C-Klep decreased with washout from 36.1 μl/g to 4.4 μl/g, much more than was expected from washout of vascular contents. Two common explanations for such large decreases are a rapid brain-to-blood efflux mechanism and reversible binding to the luminal surface of brain endothelial cells. To determine whether the remaining C-Klep was sequestered by the brain endothelial cells or had completely

crossed the BBB, we performed capillary depletion. The delta capillary/serum ratio after washout was 0.027 +/- 0.007 μl/g (n = 5) and the delta brain parenchyma/serum ratio was 1.07 +/- 0.16 (n = 5), demonstrating that some C-Klep completely crossed the BBB to enter the brain.

Ten min after icv injection, 36.6 +/- 3.6 %T (n = 9) of the C-Klep had been transported from brain (Fig 7, left panel). The value for the group receiving unlabeled Klep was 50 +/- 2.0 %T (n = 10). This was an increase of 37% and was statistically significant from the group receiving C-Klep only: $t = 3.36$, $df = 17$, $p<0.005$. C-Klep appeared in arterial serum after icv injection, confirming its brain-to-blood movement (Fig 7, right). For the C-Klep only group, 2.21 +/- 0.19 (n = 9) percent of the icv injected dose appeared in blood and for the C-Klep + unlabeled Klep group, the value was 2.78 +/- 0.21% (n = 10) of the icv injected dose. This was an increase of 26% and was not statistically significant: $0.1<p<0.05$.

Discussion

These studies were designed to investigate the uptake of a cyclodextrin by and across the BBB. We evaluated C-Klep for uptake by various regions of the brain and by peripheral tissues, for loose adherence to the luminal surface of brain capillaries, and for brain-to-blood efflux. We found that uptake was nonsaturable, suggesting that uptake was by the mechanism of transcellular diffusion. The octanol/buffer coefficient measured for C-Klep shows it to be a highly water soluble compound and the Ki for whole brain is similar to that of water soluble peptides of similar size that cross the BBB by the

mechanism of transcellular diffusion (Banks et al., 1984; Banks and Kastin, 1985). The unlabeled dose of Klep did not have a statistically significant effect on C-Klep uptake for any region of the central nervous system. However, the uptake rate varied by ten fold among brain regions, whereas the spinal cord regions after correction for vascular space showed no uptake of C-Klep. This large range among brain regions for values of Ki and the lack of uptake by the spinal cord is not typical of transcellular diffusion. Another unusual feature of the brain uptake curve was that whole brain and several brain regions rapidly came to steady state levels. We conclude that whereas transcellular diffusion is an important mechanism by which C-Klep crosses the BBB, other modifying mechanisms are also likewise at work.

One such modifying factor would be the presence of a brain-to-blood transport system. Such systems are classic causes of blood-to-brain curves rapidly reaching equilibrium and in extreme cases even giving the appearance that a substance cannot cross the BBB (Banks and Kastin, 1984; Kastin et al., 2002). If the activity of such a system varied regionally as has been shown for the BBB efflux transporter p-glycoprotein (Kannan et al., 2017), it could explain differences in retention among brain regions. We tested for an efflux system by injecting C-Klep into the lateral ventricle of the brain and determining the rate of efflux out of brain. We found that by 10 min, 36.6% of the icv injected dose available for transport had left the brain; this gives a half-time clearance from the brain of 15.2 min. This is much faster than the expected half-life of about 45 min if clearance had been only by the mechanism of CSF reabsorption (Banks et al., 1988), thus implying a brain-to-blood transporter. That C-Klep was exiting the CNS and entering the bloodstream is confirmed by the appearance of radioactivity in blood after the icv

injection. The inclusion of unlabeled Klep in the icv injection paradoxically increased the rate of efflux, rather than inhibiting it as expected in the presence of a brain-to-blood transporter. This paradox could be caused if sequestration by brain tissue is saturable or otherwise limited.

Another factor that would modify uptake would be if either the C-Klep was not fully transported across the BBB but sequestered by the capillary or if the C-Klep is only loosely adhering to the luminal surface of the capillary. The latter is a rare, but documented cause of overestimation of the rate of transport across the BBB (Triguero et al., 1990; Maness et al., 1993). Furthermore, a previous study has suggested that cyclodextrins bind to the luminal surface of capillaries with limited passage across the BBB (Pontikis et al., 2013). We used the capillary depletion method with and without washout to divide the extracellular space into three compartments: C-Klep reversibly adhering to the luminal surface, C-Klep sequestered by the brain capillaries, and C-Klep that had completely crossed the BBB. We found the majority of C-Klep was loosely adhering to the luminal surface of the capillaries, with no evidence of sequestration by the capillaries, and a small amount of C-Klep that had completely crossed the BBB.

The finding that uptake is by a nonsaturable mechanism is important in the therapeutic use of Klep. The percent of the peripherally administered dose that enters brain should be constant regardless of dose given. This simplifies the calculation of a dose that would achieve a therapeutic effect but be below that of toxicity. It also simplifies the calculation of the amount of drug in the CNS after any peripheral dose. For example, here we gave as a test for inhibition of 1 g/kg or about 30 mg/mouse. As whole brain accumulated about 0.06% of the administered dose, this would give a concentration of

21.6 μg of drug per g of whole brain. An uptake of 0.06% of the administered dose could be sufficient for some effects in brain; it is, for example, about 4 times more than the amount of morphine that accumulates in brain and in the range at which some regulatory proteins accumulate in brain (Banks and Kastin, 1994).

These findings can be put in the context of the clinical experience with Niemann-Pick disease (Calias, 2017). A dose of 10 mg/kg twice a week given into the lateral ventricle of the brain produced some measures of CNS improvement, whereas peripheral infusions of 2.5 g/kg 2-3 times per week produced minor and transient improvements (Matsuo et al., 2013; Matsuo et al., 2014). The peripheral dose/icv dose ratio is thus 250:1. This is generally an adequate ratio for a substance that has CNS effects dependent on its ability to cross the BBB. It should be noted that this ratio is lower than predicted from the % administered dose for brain (the value here of 0.06% would predict 1/0.0006 = 1,666 time the icv dose should be given) because not all of an icv dose is available to the brain. However, studies in rodents that produced robust CNS effects typically gave 4 g/kg and did so early in the life of the animal when disease was perhaps not so established. Our studies suggest, therefore, that possible reasons why peripheral dosing may be more effective in mice than in humans is that the peripheral dose given to humans is still about 2-3 times lower than needed, that the brain-to-blood efflux system in humans may be more robust than in mice, or that luminal surface sticking is higher in humans than rodents. These possibilities join the more traditional ones such as species differences in uptake and degradation, that therapy is begun later in the clinical course in humans than in laboratory animals, and species differences in brain distributions.

JPET Fast Forward. Published on July 18, 2019 as DOI: 10.1124/jpet.119.260497
This article has not been copyedited and formatted. The final version may differ from this version.

Evidence shows that the BBB is altered in lysosomal storage diseases, including increased leakiness to circulating substances (Begley et al., 2008). It may be that in the disease condition that CDs are able to take advantage of this disruption of the BBB and so more easily access the CNS.

The uptake of C-Klep by all of the peripheral tissues examined exceeded that of the vascular marker, I-Alb. All also had measureable Ki's except for heart. Given that the uptake by heart greatly exceeded that of the vascular maker I-Alb, it is likely that the unidirectional efflux phase was too short to accurately measure. The percent of the administered dose taken up per g of tissue varied among the tissues from a low for liver of 0.187 +/- 0.045 to a high for kidney of 5.90 +/- 1.57. The extremes of these two tissues is consistent with excretion of cyclodextrins being entirely by kidney (Huang et al., 2016). Only kidney showed an effect of unlabeled Klep which paradoxically increased kidney retention. This may reflect a saturable reabsorption by the kidney, which would also explain the trend towards a decrease in serum as well. However, studies with FITC-labeled cyclodextrins found no reabsorption in the proximal tubule (Huang et al., 2016).

In conclusion, we found that C-Klep can cross the BBB in small amounts and by a non-saturable mechanism. However, uptake is characterized by a very large variation among regions of the CNS and attenuated by a brain-to-blood efflux system. Furthermore, much of the apparent transport of C-Klep is actually material that is only loosely adhering to the luminal surface of the BBB. Thus, several factors determine the degree to which this cyclodextrin crosses the BBB. We conclude that the intravenous route is challenging and

to reach therapeutic levels in brain will likely require much higher peripheral doses, which could be limited by off target toxicities, or a facilitating delivery system.

JPET Fast Forward. Published on July 18, 2019 as DOI: 10.1124/jpet.119.260497
This article has not been copyedited and formatted. The final version may differ from this version.

Acknowledgements

None

Authorship Contributions:

Participated in Research Design: Banks, Engelke, Hansen, Bullock, Calias

Conducted Experiments: Hansen, Bullock

Contributed New Reagents or Analytic tools: Engelke, Calias

Performed Data Analysis: Banks, Hansen, Bullock

Wrote or Contributed to the Writing of the Manuscript: Banks, Engelke, Hansen, Bullock, Calias

References

Banks WA, Fasold MB and Kastin AJ (1997) Measurement of efflux rate from brain to blood, in *Methods in Molecular Biology: Neuropeptides Protocols* (Irvine GB and Williams CH eds) pp 353-360, Humana Press, Totowa, NJ.

Banks WA and Kastin AJ (1984) A brain-to-blood carrier-mediated transport system for small, N- tyrosinated peptides. *Pharmacology Biochemistry and Behavior* **21**:943-946.

Banks WA and Kastin AJ (1985) Peptides and the blood-brain barrier: lipophilicity as a predictor of permeability. *Brain Research Bulletin* **15**:287-292.

Banks WA and Kastin AJ (1986) Modulation of the carrier-mediated transport of the Tyr-MIF-1 across the blood-brain barrier by essential amino acids. *Journal of Pharmacology and Experimental Therapeutics* **239**:668-672.

Banks WA and Kastin AJ (1989) Quantifying carrier-mediated transport of peptides from the brain to the blood, in *Methods in Enzymology, vol 168* (Conn PM ed) pp 652-660, Academic Press, San Diego.

Banks WA and Kastin AJ (1994) Opposite direction of transport across the blood-brain barrier for Tyr-MIF-1 and MIF-1: comparison with morphine. *Peptides* **15**:23-29.

Banks WA, Kastin AJ and Coy DH (1984) Evidence that [125 I]N-Tyr-delta sleep-inducing peptide crosses the blood-brain barrier by a non-competitive mechanism. *Brain Research* **301**:201-207.

Banks WA, Kastin AJ and Fasold MB (1988) Differential effect of aluminum on the blood-brain barrier transport of peptides, technetium and albumin. *Journal of Pharmacology and Experimental Therapeutics* **244**:579-585.

Banks WA, Kastin AJ, Fischman AJ, Coy DH and Strauss SL (1986) Carrier-mediated transport of enkephalins and N-Tyr-MIF-1 across blood-brain barrier. *American Journal of Physiology* **251**:E477-E482.

Begley DJ, Pontikis CC and Scarpa M (2008) Lysosomal storage diseases and the blood-brain barrier. *Current Pharmaceutical Design* **14**:1566-1580.

Blasberg RG, Fenstermacher JD and Patlak CS (1983) Transport of alpha-aminoisobutyric acid across brain capillary and cellular membranes. *Journal of Cerebral Blood Flow and Metabolism* **3**:8-32.

Calias P (2017) 2-Hydroxypropyl-Beta-cyclodextrins and the blood-brain barrier: Considerations for Niemann-Pick disease type C1. *Curr Pharm Des* **23**:6231-6238.

Conceicao J, Adeoye O, Cabral-Marques HM and Lobo JMS (2017) Cyclodextrins as drug carriers in pharmaceutical technology: The state of the art. *Curr Pharm Des* **24**:1405-1433.

Davidson CD, Ali NF, Micsenyi MC, Stephney G, Renault S, Dobrenis K, Ory DS, Vanier MT and Walkley SU (2009) Chronic cyclodextrin treatment of murine Niemann-Pick C disease ameliorates neuronal cholesterol and glycosphingolipid storage and disease progression. *PLoS One* **4**:e6951.

Davis ME and Brewster ME (2004) Cyclodextrin-based pharmaceutics: past, present, and future. *Nat Rev Drug Discov* **3**:1023-1035.

el Tayar N, Tsai RS, Testa B, Carrupt PA and Leo A (1991) Partitioning of solutes in different solvent systems: the contribution of hydrogen-bonding capacity and polarity. *J Pharm Sci* **80**:590-598.

Frey WH, II (2002) Bypassing the blood-brain barrier to deliver therapeutic agents to the brain and spinal cord. *Drug Delivery Technology* **2**:46-49.

Gil ES, Wu L, Xu L and Lowe TL (2012) Beta-cyclodextrin-poly(Beta-amino ester) nanoparticles for sustained drug delivery across the blood-brain barrier. *Biomacromolecules* **13**:3533-3541.

Huang J, Weinfurter S, Pinto PC, Pretze M, Kranzlin B, Pill J, Federica R, Perciaccante R, Ciana LD, Masereeuw R and Gretz N (2016) Flourescently labeled cyclodextrin derivatives as exogenous markers for real-time transcutaneous measurement of renal function. *Bioconjug Chem* **27**:2513-2526.

Kannan P, Schain M, Kretzschmar WW, Weidner L, Mitsios N, Gulyas B, Blom H, Gottesman MM, Innis RB, Hall MD and Mulder J (2017) An automated method measures variability in P-glycoprotein and ABCG2 densities across brain regions and brain matter. *J Cereb Blood Flow Metab* **37**:2062-2075.

Kastin AJ, Fasold MB and Zadina JE (2002) Endomorphins, Met-enkephalin, Tyr-MIF-1 and the P-glycoprotein efflux system. *Drug Metabolism and Disposition* **30**:231-234.

Liu B, Turley SD, Burns DK, Miller AM, J.J. R and Dietschy JM (2009) Reversal of defective lysosomal transport in NPS disease ameliorates liver dysfunction and neurodegneration in the npc1-/- mouse. *Proc Natl Acad Sci USA* **17**:2377-2382.

Loftsson T and Brewster ME (2010) Pharmaceutical applications of cyclodextrins: basic science and product development. *J of Pharmacy and Pharmacology* **62**:1607-1621.

Maness LM, Banks WA, Podlisny MB, Selkoe DJ and Kastin AJ (1994) Passage of human amyloid ·-protein 1-40 across the murine blood-brain barrier. *Life Sciences* **21**:1643-1650.

Maness LM, Kastin AJ, Banks WA, Banks MF, Podlisny MB and Selkoe DJ (1993) Passage of human ·-amyloid 1-40 across the murine blood-brain barrier. *Society for Neuroscience Abstracts* **19**:696.

Matsuo M, Shraishi K, Wada K, Ishitsuka Y, Doi H, Maeda M, Mizoguchi T, Eto J, Mochinaga S, Arima H and Irie T (2014) Effects of intracerebroventricular administration of 2-hydroxypropyl-beta-cyclodextrin in a patient with Niemann-Pick type C disease. *Mol Genet Metab Rep* **17**:391-400.

Matsuo M, Togawa M, Hirabaru K, Mochinaga S, Narita A, Adachi M, Egashira M, Irie T and Ohno K (2013) Effects of cyclodextrin in two patients with Niemann-Pick Type C disease. *Mol Genet Metab* **108**:76-81.

Monnaert V, Tilloy S, Bricout H, Fenart L, Cecchelli R and Monflier E (2004) Behavior of alpha-, beta-, and gamma-cyclodextrins and their derivatives on an in vitro model of the blood-brain barrier. *J Pharmacol Exp Therap* **310**:745-751.

Nonaka N, Farr SA, Kageyama H, Shioda S and Banks WA (2008) Delivery of galanin-like peptide to the brain: Targeting with intranasal delivery and

cyclodextrins. *Journal of Pharmacology and Experimental Therapeutics* **325:**:513-519.

Nonaka N, Farr SA, Nakamachi T, Morley JE, Nakamura M, Shioda S and Banks WA (2012) Intranasal administration of PACAP: Uptake by brain and regional brain targeting with cyclodextrins. *Peptides* **36**:168-175.

Patlak CS, Blasberg RG and Fenstermacher JD (1983) Graphical evaluation of blood-to-brain transfer constants from multiple-time uptake data. *Journal of Cerebral Blood Flow and Metabolism* **3**:1-7.

Pontikis CC, Davidson CD, Walkley SU, Platt FM and Begley DJ (2013) Cyclodextrin alleviates neuronal storage of cholesterol in Niemann-Pick C disease without evidence of detectable blood-brain barrier permeability. *J Inherit Metab Dis* **36**:491-498.

Soares AF, de Albuquerque Carvalho R and Veiga F (2007) Oral administration of peptides and proteins: nanoparticles and cyclodextrins as biocompatible delivery systems. *Nanomedicine* **2**:183-202.

Triguero D, Buciak J and Pardridge WM (1990) Capillary depletion method for quantification of blood-brain barrier transport of circulating peptides and plasma proteins. *Journal of Neurochemistry* **54**:1882-1888.

Varca GHC, Andreo-Fiho N, Lopes PS and Ferraz HG (2010) Cyclodextrins: An overview of the complexation of pharmaceutical proteins. *Current Protein and Peptide Science* **11**:255-263.

Footnotes:
Funded by Veterans Affairs

JPET Fast Forward. Published on July 18, 2019 as DOI: 10.1124/jpet.119.260497
This article has not been copyedited and formatted. The final version may differ from this version.

Figure Legends

Figure 1. Clearance of C-Klep from Circulation After Intravenous Injection. Top Panel: Clearance of C-Klep expressed as %Inj/ml vs time showed two phases. Bottom Panel: Clearance using log(%Inj/ml) vs time shows early distribution phase with half-time disappearance of 15.7 min followed by a plateau. N = 18 for both panels.

Figure 2. Uptake of C-Klep by Whole Brain. Top Panel: Uptake was linear for the first 15-20 min after intravenous injection, yielding a unidirectional influx rate of 0.236 +/- 0.057 μl/g-min. Lower Panel: Uptake expressed as %Inj/g followed a hyperbolic pattern, reaching a theoretical maximum of .072 +/- 0.006 %Inj/g. N = 18 for both panels.

Figure 3. Uptake of C-Klep by Brain Region. All regions took up C-Klep, but uptake varied by over 10 fold among the regions. The hypothalamus with a Ki of 0.757 +/- 0.155 μl/g-min had the fastest uptake and the region with the slowest uptake was the frontal cortex with a Ki of 0.062 +/- 0.018 μl/g-min. N = 18 per panel.

Figure 4. Uptake of C-Klep by Peripheral Tissues. All tissues showed a significant correlation between tissue/serum ratios vs time except for heart. The dashed line shows the vascular space for the tissue as measured by radioactive albumin. N = 18 per panel.

Figure 5. The Percent of the Injected Dose Taken up per Gram of Tissue. Upper panel shows results for brain regions. Lower panel shows results for peripheral tissues. N = 18 per group.

Figure 6. Effects of Unlabeled Kleptose on Uptake by Brain, Serum, Liver, and Kidney. No evidence for saturable uptake was found for any tissue. However, a paradoxic increase for kidney and a trend for a decrease in serum was found. N = 8 for kidney; n = 10 for all other groups.

Figure 7. Brain-to-Blood Efflux of C-Klep After Its Intracerebroventricular (icv) Injection. Left hand panel shows percent of the icv injected material that was transported out of brain based on residual levels in brain of radioactivity. Right hand panel shows appearance of the icv injection radioactivity in carotid artery serum. Both figures are consistent with increased efflux when C-Klep was co-injected with unlabeled kleptose. N = 10/group.

JPET Fast Forward. Published on July 18, 2019 as DOI: 10.1124/jpet.119.260497
This article has not been copyedited and formatted. The final version may differ from this version.

Table I. Unidirectional Influx Rates for C-Klep.

Tissue	Ki +/-SE (microl/g-min)	Vi +/- SE (microl/g)	n	R2	p<
Olfactory Bulb	0.413 +/- 0.137	29.5 +/- 2.2	18	0.361	0.01
Whole Brain	0.235 +/- 0.057	11.3 +/- 0.42	14	0.586	0.005
Frontal Cortex	0.062 +/- 0.018	9.05 +/- 0.30	18	0.410	0.005
Parietal Cortex	0.110 +/- 0.040	10.6 +/- 0.66	18	0.317	0.05
Occipital Cortex	0.708 +/- 0.175	11.7 +/- 1.3	14	0.578	0.005
Hippocampus	0.101 +/- 0.035	10.4 +/- 0.6	17	0.356	0.05
Hypothalamus	0.757 +/- 0.155	16.4 +/- 1.8	16	0.629	0.001
Thalamus	0.235 +/- 0.059	8.57 +/- 0.43	14	0.567	0.005
Striatum	0.202 +/- 0.058	12.2 +/- 0.9	18	0.434	0.005
Cerebellum	0.330 +/- 0.095	13.4 +/- 0.7	14	0.499	0.005
Midbrain	0.382 +/- 0.096	10.6 +/- 0.7	14	0.569	0.005
Pons-Medulla	0.156 +/- 0.033	17.1 +/- 0.5	18	0.584	0.001
Cervical SC	0.365 +/- 0.113	15.9 +/- 1.8	18	0.403	0.005
Thoracic SC	0.0893 +/- 0.019	5.98 +/- 0.31	18	0.584	0.001
Lumbar SC	0.177 +/- 0.052	9.95 +/- 0.85	18	0.421	0.005
Spleen	0.654 +/- 0.181	111 +/- 3	18	0.449	0.005
Lung	26.9 +/- 7.0	236 +/- 18	6	0.785	0.05
Kidney	7.72 +/- 2.63	200 +/- 38	16	0.381	0.05

Liver	7.97 +/- 2.75	66.2 +/- 7.0	6	0.677	0.05
Heart	0.537 +/- 0.347	193 +/- 6	18	0.130	NS
G Muscle	6.14 +/- 1.14	55.8 +/- 6.3	12	0.745	0.001

NS: not statistically significant.

Table II. Vascular Space as Measured by Albumin.

Tissue	microl/g*		Tissue	microl/g*
Olfactory Bulb	19.6 +/- 1.7		Cervical SC	23.9 +/- 3.3
Whole Brain	11.3 +/- 0.8		Thoracic SC	8.6 +/- 1.0
Frontal Cortex	9.5 +/- 0.7		Lumbar SC	11.5 +/- 2.2
Parietal Cortex	10.0 +/- 1.3			
Occipital Cortex	13.7 +/- 1.5		Spleen	78.0 +/- 5.2
Hippocampus	10.2 +/- 0.5		Lung	212.5 +/- 26.8
Hypothalamus	14.2 +/- 1.5		Kidney	92.0 +/- 4.9
Thalamus	8.1 +/- 0.3		Liver	77.1 +/- 4.5
Striatum	12.1 +/- 2.0		Heart	122.3 +/- 3.3
Cerebellum	13.7 +/- 1.9		G Musc	12.8 +/- 0.8
Midbrain	12.4 +/- 0.9			
Pons Medulla	14.2 +/- 0.7			

*mean +/-SE, n = 6; SC = Spinal Cord; G Musc = Gastrocnemius Muscle

Table 3. Brain/serum ratios for C-Klep with and without washout of the brain vascular space.

	No Washout (n = 9)	Washout (n = 10)
Tc-Alb	9.7 +/- 0.2	0.8 +/- 0.1
C-Klep	36.1 +/- 2.0	4.4 +/- 0.2

Means +/- SE; units in microl/g.

JPET Fast Forward. Published on July 18, 2019 as DOI: 10.1124/jpet.119.260497
This article has not been copyedited and formatted. The final version may differ from this version.

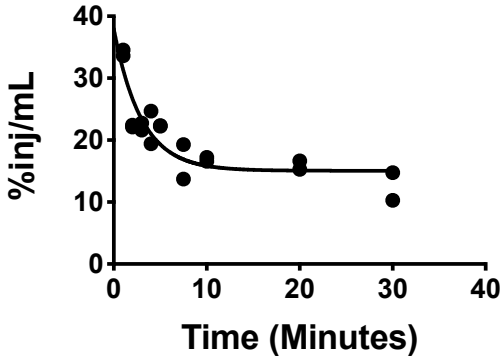

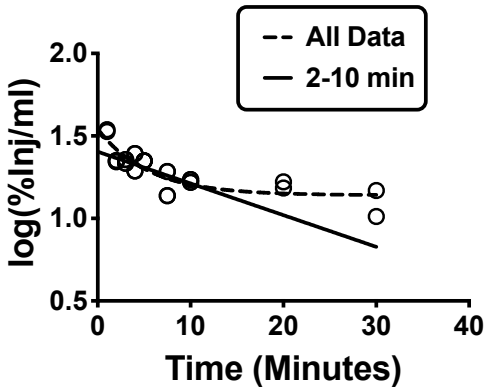

Fig 1

JPET Fast Forward. Published on July 18, 2019 as DOI: 10.1124/jpet.119.260497
This article has not been copyedited and formatted. The final version may differ from this version.

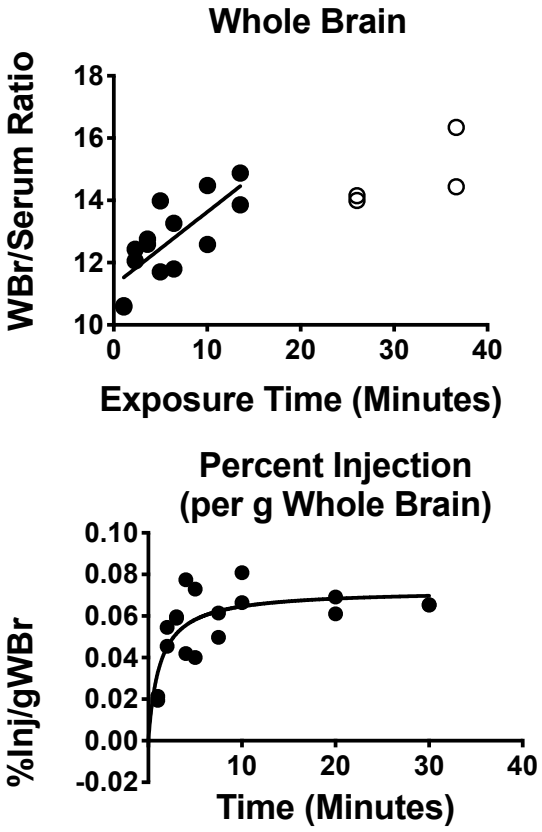

Fig 2

JPET Fast Forward. Published on July 18, 2019 as DOI: 10.1124/jpet.119.260497
This article has not been copyedited and formatted. The final version may differ from this version.

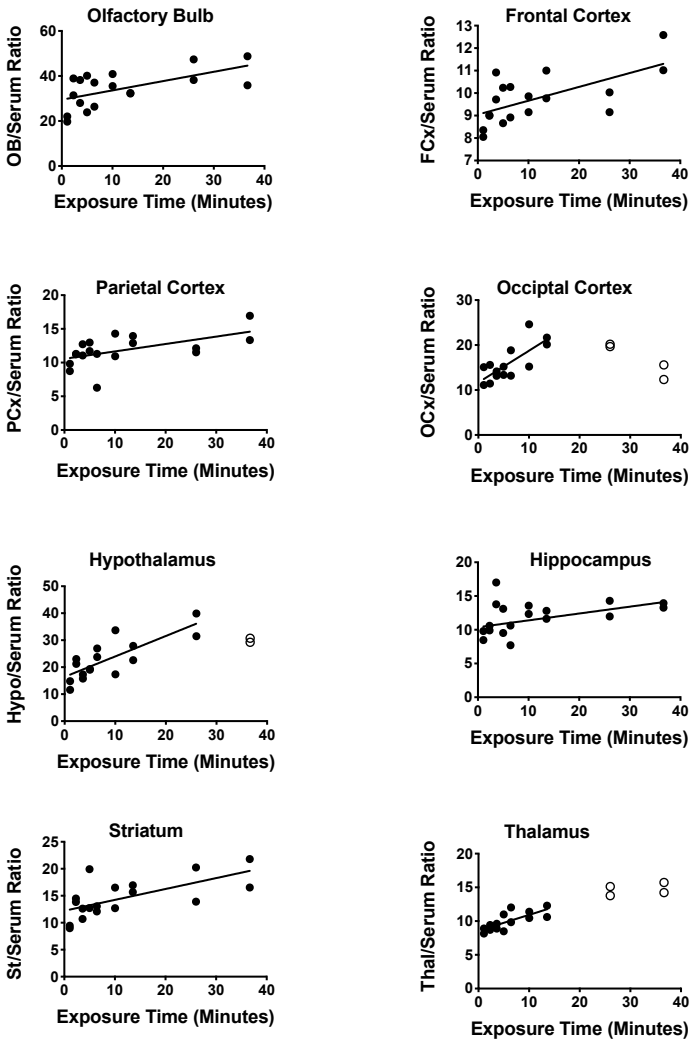

Fig 3

JPET Fast Forward. Published on July 18, 2019 as DOI: 10.1124/jpet.119.260497
This article has not been copyedited and formatted. The final version may differ from this version.

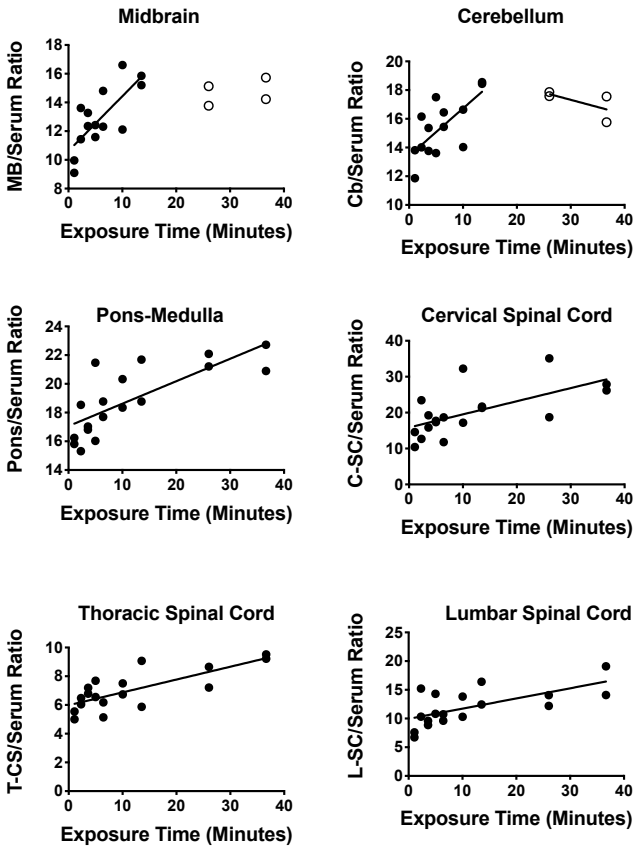

Fig 3 cont

JPET Fast Forward. Published on July 18, 2019 as DOI: 10.1124/jpet.119.260497
This article has not been copyedited and formatted. The final version may differ from this version.

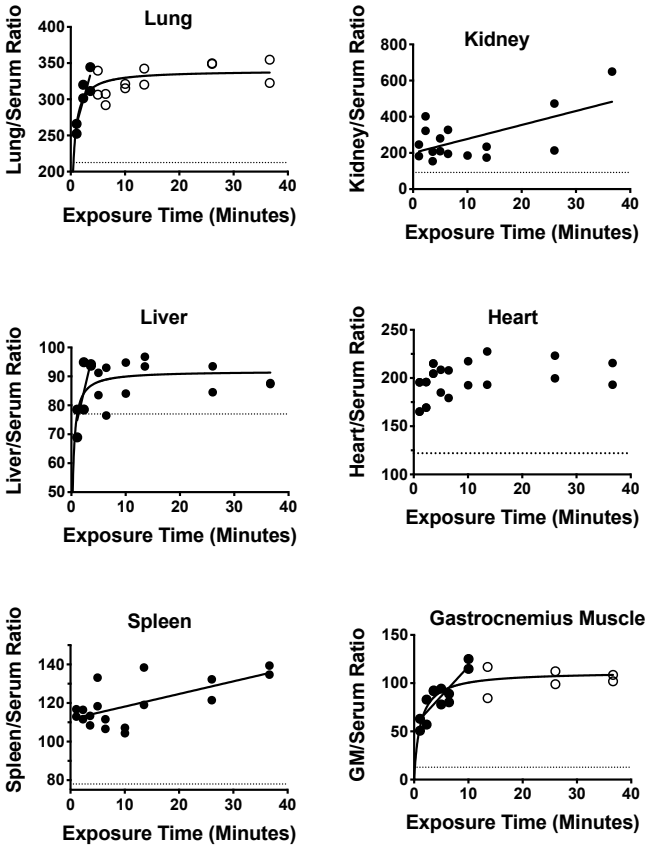

Fig 4

JPET Fast Forward. Published on July 18, 2019 as DOI: 10.1124/jpet.119.260497
This article has not been copyedited and formatted. The final version may differ from this version.

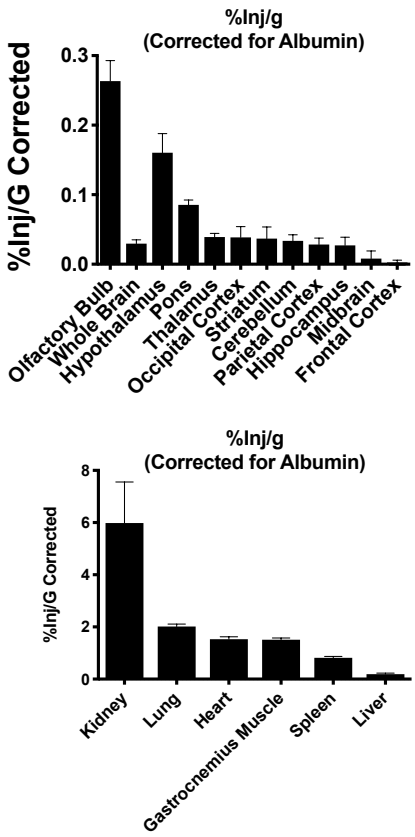

Fig 5

JPET Fast Forward. Published on July 18, 2019 as DOI: 10.1124/jpet.119.260497
This article has not been copyedited and formatted. The final version may differ from this version.

Figure 6

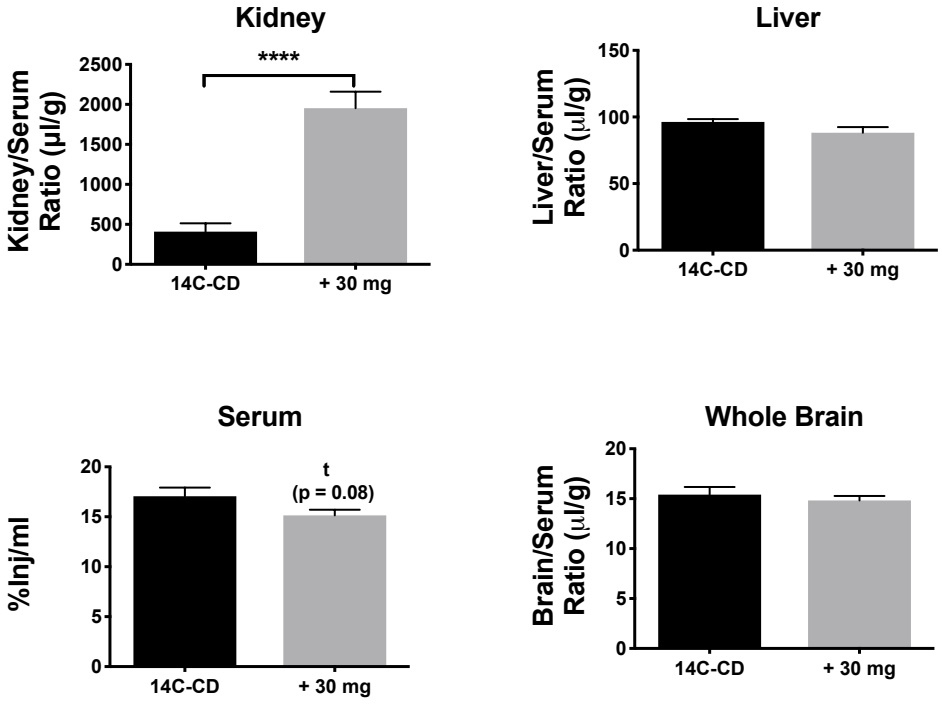

JPET Fast Forward. Published on July 18, 2019 as DOI: 10.1124/jpet.119.260497
This article has not been copyedited and formatted. The final version may differ from this version.

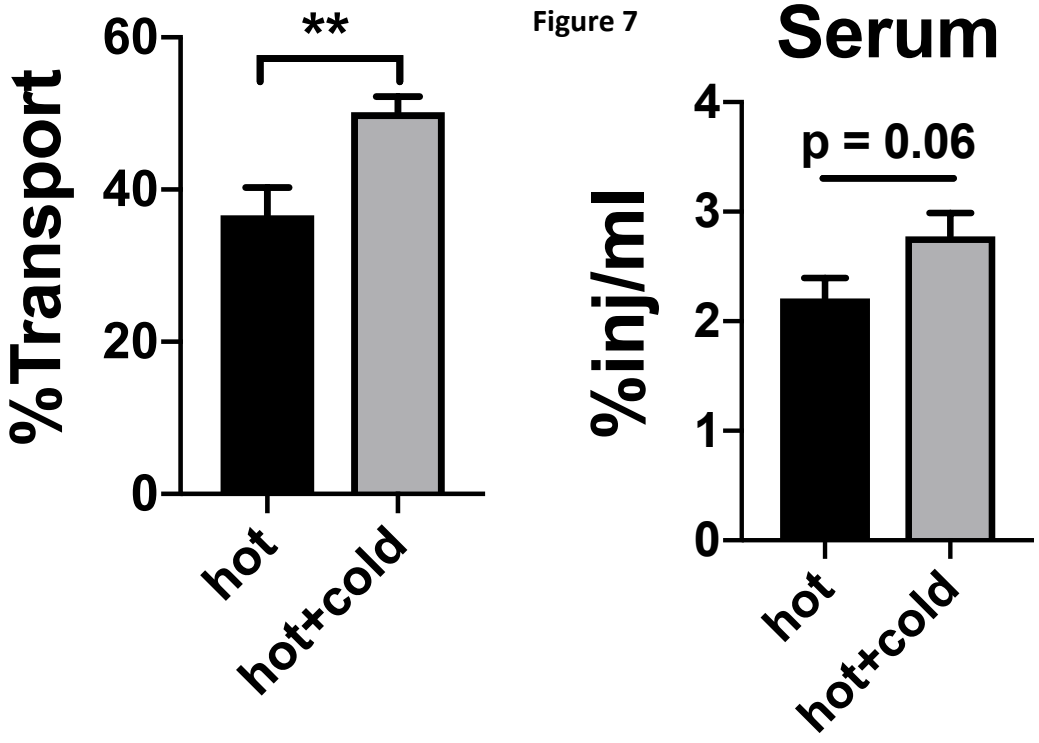

Figure 7